Evaluation of [^{99m}Tc-(CO)$_3$-X-Y-Bombesin(7-14)NH$_2$] Conjugates for Targeting Gastrin-releasing Peptide Receptors Overexpressed on Breast Carcinoma

LAUREN B. RETZLOFF[1,3], LAURA HEINZKE[3], SAID D. FIGUREOA[2,7], SAMANTHA V. SUBLETT[7], LIXIN MA[2,4,7], GARY L. SIECKMAN[7], TAMMY L. ROLD[3,7], ISABEL SANTOS[8], TIMOTHY J. HOFFMAN[3,6,7] and CHARLES J. SMITH[2,3,5,6,7]

Departments of [1]Medical Pharmacology and Physiology, [2]Radiology and [3]Internal Medicine, [4]International Institute of Nano and Molecular Medicine, [5]Research Reactor, and [6]Radiopharmaceutical Sciences Institute, University of Missouri, Columbia, MO 65211, U.S.A.; [7]Research Division, Harry S. Truman Memorial Veterans' Hospital, Columbia, MO 65201, U.S.A.; [8]Department of Chemistry, Technological and Nuclear Institute, 2686-953 Sacavém, Portugal

Abstract. *Background: Gastrin-releasing peptide (GRP) receptors are overexpressed on a variety of human carcinomas, including those of the breast. These receptors may be targeted with bombesin (BBN), which binds to GRP receptors with high affinity and specificity. The aim of this study was to develop a ^{99m}Tc(I)-BBN analog with favorable pharmacokinetic properties in order to improve the visualization of breast cancer tissue. Materials and Methods: Solid-phase peptide synthesis was used to produce a series of X-Y-BBN-NH2 conjugates, where X is pyrazolyl (PZ1) or 2,3-diaminopropionic acid (DPR) and Y is a spacer sequence. Their metallated counterparts were prepared by reacting [^{99m}Tc-(H$_2$O)$_3$(CO)$_3$]$^+$ with the corresponding ligand. Results: While the PZ1 conjugates exhibited higher GRP receptor binding affinities in vitro, the DPR analogs demonstrated superior target tissue accumulation and pharmacokinetic properties in vivo. Conclusion: These results demonstrate the ability of the DPR derivatives (Y=glycylserylglycine, triserine) to clearly identify the T47-D tumor tissue in xenografted SCID mice.*

Among women in the United States, breast cancer is the most common form of cancer and the second leading cause of cancer death (1). For the average woman, this translates into a 1 in 8 lifetime chance of developing invasive breast cancer, and a 1 in 33 chance of breast cancer causing her death (1). This trend is expected to continue into 2009, with the diagnosis of an estimated 256,560 new cases (194,280 invasive, 62,280 *in situ*) and 40,610 deaths (1). While mammography is an effective tool for the early diagnosis of primary breast cancer in many patients, it has considerable limitations when imaging women with breast implants, post-surgical recurrence, or dense breast tissue (1, 2). As a result, there is considerable interest in the development of novel modalities that may be employed to image primary breast carcinoma (2-10). Among these, nuclear imaging is ideally suited for this task as it targets various physiological features that are characteristic of human cancer cells, including receptor overexpression, increased metabolic rate, and angiogenesis.

Current research in the field of nuclear imaging has focused on the development of radiolabeled peptides that selectively target receptors uniquely overexpressed on human cancer cells (11, 12). For breast carcinomas, a number of potential receptor targets have been investigated including somatostatin receptors (SST_{2A}), neuropeptide Y receptors ($NPYY_1$), and gastrin-releasing peptide (GRP) receptors (13-15). The SST_{2A} receptor was the focus of many early studies as it is expressed in 50-70% of *in vitro* breast cancer specimens and may be targeted using the commercially available radiotracer Octreoscan® (14). However, *in vivo* the SST_{2A} receptor is present at a low density (<2,000 dpm/mg tissue) and is heterogeneously distributed among breast cancer cells (14). This results in an insufficient signal for imaging purposes and precludes the use of somatostatin as a receptor target for routine breast cancer diagnosis. In order to avoid these problems, current research has focused on receptor targets that are present at a high density (>2,000 dpm/mg tissue) on the majority of breast carcinomas (14-16).

Correspondence to: Dr. C. Jeffrey Smith, Radiopharmaceutical Sciences Institute, 143 Major Hall, University of Missouri, Columbia, MO 65211, U.S.A. Tel: +1 573 814 6000 ext. 3683, Fax: +1 573 882-1663, e-mail: smithcj@mail.missouri.edu

Key Words: Breast cancer, technetium, GRP receptor, carbonyl, T47-D, MDA-MB-231.

For example, in a study conducted by Gugger *et al*., 69% (53/77) of the breast cancer specimens analyzed expressed the NPY(Y_1) receptor (14). This expression was determined to be high in 58% (45/77) of the samples, with a mean receptor density of 9,135±579 dpm/mg tissue (14). In the same study, the GRP receptor was determined to be present in 71% (55/77) of the samples tested, and in 65% of these cases, GRP receptor expression was categorized as high (mean receptor density 9,819±530 dpm/mg tissue) (14). In addition, the lymph node metastases from patients with GRP receptor-positive primary breast carcinomas demonstrate a similar receptor expression profile, indicating that a GRP receptor-targeting radiopharmaceutical may potentially be used to image both the primary tumor and any metastatic sites (14). Indeed, both Scopinaro *et al*. and Van de Wiele *et al*. have obtained such images in breast cancer patients using technetium-99m (^{99m}Tc)-labeled GRP receptor-targeted radiotracers (9, 10). Thus, the GRP receptor should be considered a potential target for the development of radiopharmaceuticals designed to image breast carcinoma.

Effective targeting of the GRP receptor may be accomplished using bombesin (BBN), a tetradecapeptide, initially isolated from the skin of a tree frog, that binds the GRP receptor with high affinity and specificity (17-20). BBN analogs have been radiolabeled with various radioactive metals for imaging of GRP receptor-positive tumors in both rodents and humans (2, 9, 10, 18). Among these metals, ^{99m}Tc is frequently selected when designing radiotracers for single photon-emission computed tomography (SPECT) imaging due to its ideal decay characteristics (~89% IT, 140.5 keV γ, $t_{1/2}$=6.01 hours), onsite availability (^{99}Mo/^{99m}Tc generator), and diverse labeling chemistry (2, 12, 21). Current research has focused on the development of organometallic, tricarbonyl-based technetium radiopharmaceuticals due to the kinetic inertness conferred to Tc(I) by the presence of low spin d^6 electrons, as well as the ease with which these compounds may be synthesized using the Isolink® radiolabeling kit (21-23). The aqua ion complex, $[^{99m}Tc\text{-}(H_2O)_3(CO)_3]^+$ that is produced may be effectively stabilized *in vivo* by either bi- or tridentate ligand frameworks that are composed of primary, secondary, or aromatic amines (21, 23, 24).

In this study, we report on the synthesis, characterization, and ^{99m}Tc radiometallation of a series of pyrazolyl (PZ1)-Y-BBN(7-14)NH_2 and 2,3-diaminopropionic acid (DPR)-Y-BBN(7-14)NH_2-based targeting vectors with high affinity and specificity for the mammalian GRP receptor. These conjugates underwent *in vitro* competitive displacement and internalization-externalization analysis in both T47-D and MDA-MB-231 human breast cancer cell lines prior to *in vivo* evaluation in CF-1 and T47-D tumor bearing SCID mice. Results from these experiments were used to select the most promising analogs for molecular imaging studies in T47-D tumor-bearing SCID mice.

Materials and Methods

Solvents were purchased from Fisher Scientific (Pittsburg, PA, USA) and used without further purification. Fmoc-amino acids, coupling reagents, and resin were purchased from Calbiochem-Novabiochem Corp. (San Diego, CA, USA). All other reagents were purchased from Fisher Scientific, Sigma-Aldrich Chemical Company (St. Louis, MO, USA), or ACROS Organics (Geel, Belgium) and used without further purification. ^{125}I-Tyr^4-BBN was purchased from Perkin Elmer (Waltham, MA, USA). $^{99m}TcO_4$ was obtained as a sterile 0.9% aqueous NaCl eluant from a ^{99}Mo/^{99m}Tc generator (Bristol-Meyers Squibb, New York, NY, USA).

Reverse-phase high-performance liquid chromatographic (RP-HPLC) purification and analyses of all conjugates and their metallated complexes were performed on an SCL-10A HPLC system (Shimadzu, Kyoto, Japan) using a binary gradient system (solvent A=99.9% deionized (DI) water, 0.1% trifluoroacetic acid (TFA); solvent B=99.9% acetonitrile (ACN), 0.1% TFA). This system was equipped with an in-line SPD-10A UV-visible absorption detector (Shimadzu; λ=280 nm), an in-line ORTEC NaI solid crystal scintillation detector (EG & G, Salem, MA, USA), an Eppendorf CH-30 column heater (34˚C; Hamburg, Germany), and a reversed-phase column (Phenomenex, Belmont, CA, USA). EZStart software (7.3; Shimadzu) was used for data acquisition of both signals.

Conjugate synthesis and purification. Rink amide resin (53.2 mg) and Fmoc-protected amino acids and spacer groups were used for solid phase peptide synthesis of the non-metallated BBN conjugates. The sequential addition of amino acids was accomplished by reacting O-benzotriazole-N,N,N',N'-tetramethyl-uronium-hexafluoro-phosphate (HBTU) activated carboxyl groups on the reactant with the *N*-terminal amino group on the growing peptide, anchored *via* the *C*-terminus to the resin. The peptide sequence was selected to produce analogs with the following general structure: X-Y-Q-W-A-V-G-H-L-M-NH_2, where X indicates PZ1 or DPR, and Y indicates the spacer group β-alanine (βAla), triglycine (GGG), glycylserylglycine (GSG), Peg5, Peg8, serylglycylserine (SGS), or triserine (SSS). The peptide products were cleaved by a standard procedure employing a cocktail of thioanisol, water, ethanedithiol, and TFA (2:1:1:36) followed by precipitation into methyl-*t*-butyl ether. The crude peptides were purified by RP-HPLC using a semi-preparative C-18 reversed phase column (250×10 mm, 10 μm). The mobile phase solvent composition was shifted from 95%A:5%B to 1%A:99%B over a 25-minute gradient at a flow rate of 5.0 ml/min to achieve separation. Solvents were removed using a CentriVap system (Labconco, Kansas City, MO, USA). Electrospray ionization mass spectrometry (ESI-MS) (SynPep; Dublin, CA, USA, or University of Missouri-Columbia Proteomics Center, Columbia, MO, USA) was employed to characterize all X-Y-BBN(7-14)NH_2 conjugates.

^{99m}Tc-radiolabeling. The $^{99m}Tc\text{-}(CO)_3$-X-Y-BBN(7-14)NH_2 analogs were prepared in high radiochemical yield (~95%) *via* the addition of $[^{99m}Tc\text{-}(H_2O)_3(CO)_3]^+$ (Isolink® kit; Tyco Healthcare, St. Louis, MO, USA) to a vial containing 100 μg of conjugate dissolved in 100 μl of water. The yield of radiolabeled conjugate was maximized by adjusting the pH to 7 using 0.1 M HCl prior to heating at 80˚C for 1 hour. After incubation, the metallated complexes were purified by RP-HPLC and the peaks collected into either 100 μl of DI H_2O containing 100 μg of bovine serum albumin solution (BSA, *in vitro*

analysis) or 100 µl of isotonic saline (*in vivo* analysis). Residual ACN was evaporated from the solution using a stream of nitrogen.

In vitro analysis. Purified radioconjugate (100 µl) was added to either 900 µl of 10^{-3} M histidine solution in phosphate-buffered saline (PBS, pH=7.4) or 300 µl human serum albumin (HSA). The samples were incubated at room temperature (histidine challenge) or at 37˚C (5% CO_2, HSA challenge) until RP-HPLC analysis at 1, 3, and 5 hours. This analysis was performed using an analytical C-18 reversed phase column (250×4.6 mm, 4 µm). The mobile phase solvent composition was shifted from 95%A:5%B to 10%A:90%B over a 28-minute gradient at a flow rate of 1.5 ml/min.

The binding affinity of each analog was assessed using a competitive radioligand binding assay (n=3) (25). Approximately 3×10^6 MBA-MD-231 or 3×10^5 T47-D human breast cancer cells (ATCC, Manassas, VA, USA) suspended in 300 µl RPMI-1640 media containing 4.8 mg/ml HEPES, 0.1 µg/ml bacitracin, and 2 mg/ml BSA (pH=7.4) were incubated at 37˚C (5% CO_2) for 40 minutes in the presence of 20,000 cpm of 125I-Tyr^4-BBN and increasing concentrations of non-metallated conjugate. After incubation, the reaction medium was aspirated and the cells were washed with media (4×). Cell-associated radioactivity was determined by counting in a Packard Riastar gamma counting system. The percentage of ^{125}I-Tyr^4-BBN(7-14)NH_2 bound to the cells was plotted *versus* the concentration of each conjugate to determine the various 50% inhibitory concentration (IC_{50}) values.

In vitro studies were performed to evaluate the extent of internalization and subsequent residualization of ^{99m}Tc as a function of time (n=3) (26). Approximately 3×10^6 MDA-MB-231 or 3×10^5 T47-D human breast cancer cells suspended in 300 µl RPMI-1640 media containing 4.8 mg/ml HEPES, 0.1 µg/ml bacitracin, and 2 mg/ml BSA (pH=7.4) were incubated in the presence of 20,000 cpm metallated conjugate at 37˚C (5% CO_2) until sampling. For internalization analysis, sampling was performed at 15, 30, 45, 60, 90, and 120 minutes. For externalization analysis, analogs underwent a 40-minute incubation period to allow for conjugate internalization. After this initial incubation period, the reaction medium was aspirated and the cells were washed with warm media. The cells were resuspended in media and placed in the incubator until sampling at 15, 30, 45, 60, and 90 minutes. At the time of sampling, the reaction medium was aspirated and the cells were washed with media (4×). Surface-bound radioactivity was removed by washing the cells with cold (4˚C) 0.2 N acetic acid/0.5 M NaCl (pH=2.5). The percentage of internalized cell-associated radioactivity as a function of time was determined by counting in a Packard Riastar gamma counting system.

In vivo biodistribution. Biodistribution studies were performed in both CF-1 mice and severe combined immunodeficient (SCID) mice bearing T47-D tumor xenografts (n=5). Four- to five-week-old female CF-1 and ICR SCID outbred mice were obtained from Taconic (Germantown, NY, USA). The mice were housed in sterile micro-isolator cages (5 animals/cage) in a temperature- and humidity-controlled room with a 12-hour light/12-hour dark schedule. The animals were fed autoclaved rodent chow (Rawlston Purina Company, St. Louis, MO, USA) and water *ad libitum*. SCID mice were housed one week prior to estradiol implants and transplantation of tumor cells. Animals were anesthetized for injections with isoflurane (Baxter Healthcare Corporation, Deerfield, IL, USA) at a rate of 2.5% with 0.4 l oxygen through a non-rebreathing anesthesia vaporizer.

Mice receiving T47-D tumor xenografts were administered β-estradiol supplementation (1.7 mg/pellet) (Innovative Research of America, Sarasota, FL, USA) by making a small incision, and implanting a 3 mm pellet subcutaneously between the shoulder blades. The incision was closed with Vetbond tissue adhesive (3M Animal Care Products, St. Paul, MN, USA). Approximately 5×10^6 T47-D human breast ductal carcinoma cells suspended in a 100 µl solution of normal sterile saline and Matrigel (1:1) (BD Biosciences, San Jose, CA, USA) were injected on the bilateral subcutaneous flanks and allowed to proliferate *in vivo* for nine weeks post-inoculation (*p.i.*). At the end of this period, tumors had developed that ranged in weight from 0.01 to 0.41 g.

Mice were injected with either 5 µCi (1 and 4 hours) or 10 µCi (24 hours) of ^{99m}Tc-$(CO)_3$-X-Y-BBN(7-14)NH_2 conjugate in 50 µl of isotonic saline *via* the tail vein. At 1, 4, and 24 hours *p.i.*, mice were euthanized and their tissues and organs were excised, weighed, and the associated radioactivity counted in a Packard Riastar gamma counting system. The percentage injected dose (%ID) and %ID/g of each organ or tissue were calculated. The %ID in whole blood was estimated assuming a whole-blood volume of 6.5% the total body weight.

In vivo imaging. Imaging studies for the ^{99m}Tc-$(H_2O)(CO)_3$-DPR-GSG-BBN(7-14)NH_2 and the ^{99m}Tc-$(H_2O)(CO)_3$-DPR-SSS-BBN(7-14)NH_2 analogs were performed in SCID mice bearing T47-D tumors. Mice were injected with approximately 5 mCi conjugate in 200 µl of isotonic saline *via* the tail vein. At 24 hours *p.i.*, mice were euthanized by CO_2 administration and placed in a prone position on a custom-built cradle mounted with image fusion markers to serve as reference points for subsequent SPECT/CT/MRI image co-registration.

A Micro-CAT II SPECT/CT unit (Siemens Medical Solution Incorporated, TN, USA) equipped with dual pixellated NaI detectors, 2 mm pinhole collimators, a CCD x-ray detector, and an 80 kVp microfocus x-ray source (40 µm focal spot) was employed for SPECT and CT image acquisition. Volumetric SPECT data were generated with a 3-dimensional ordered-subsets expectation maximization (OSEM) algorithm with geometric misalignment corrections. SPECT image reconstruction used 12 iterations and 4 subsets. Concurrent microCT whole-body imaging was performed to allow for fusion of anatomic and molecular data. Magnetic resonance imaging (MRI) was performed using a 7 T/210 mm Varian Unity Inova MRI system equipped with a quadrature driven birdcage coil (38 mm I.D.) (Varian Incorporated, Palo Alto, CA, USA) in order to correlate relative ^{99m}Tc$(H_2O)(CO)_3$-DPR-Y-BBN[7-14]NH_2 conjugate uptake with anatomical structures. Coronal images were acquired using a fast-spin echo-multi-slice (FSEMS) sequence. The Amira 3.1 software package (TGS, Mercury Computer Systems, Germany) was employed for co-registration, visualization, and analysis of the SPET/CT/MRI data. All animal studies were conducted in accordance with the highest standards of care as outlined in the NIH guide for Care and Use of Laboratory Animals and the Policy and Procedures for Animal Research at the Harry S. Truman Memorial Veterans' Hospital.

Results

Synthesis and radiolabeling. A series of X-Y-BBN(7-14)NH_2 conjugates, where X=PZ1 or DPR, and Y=βAla, GGG, GSG, Peg5, Peg8, SGS, or SSS, were synthesized by solid-phase peptide synthesis in yields of approximately 70% after RP-HPLC purification. Reverse-phase chromatograms of these

Table I. *X-Y-BBN[7-14]NH$_2$ ESI-MS and IC$_{50}$ data (*n=3).*

X-Y-BBN	ESI-MS (m/z)		IC$_{50}$ nmol (SD) T47-D*	IC$_{50}$ nmol (SD) MDA-MB-231*
	Calculated	Observed		
PZ1-βAla	1261.54	1261.69	0.71 (1.86)	0.33 (1.89)
PZ1-GGG	1361.62	1361.71	6.12 (2.97)	2.01 (1.01)
PZ1-Peg5	1376.67	1376.75	1.99 (1.87)	0.65 (0.52)
PZ1-Peg8	1420.72	1420.70	3.15 (3.50)	0.78 (1.30)
PZ1-SSS	1451.69	1452.50	1.39 (0.62)	0.54 (2.16)
DPR-βAla	1097.29	1096.56	2.01 (1.11)	1.08 (1.72)
DPR-GSG	1227.40	1226.60	8.09 (1.25)	6.11 (1.51)
DPR-SGS	1257.42	1256.70	0.79 (2.10)	0.26 (1.57)
DPR-SSS	1287.45	1286.67	5.86 (0.83)	2.22 (1.19)

Table II. *Non-metallated and metallated X-Y-BBN[7-14]NH$_2$ RP-HPLC data.*

X-Y-BBN	Retention time (min)	
	Non-metallated	Metallated
PZ1-βAla	13.45	17.26
PZ1-GGG	13.08	16.40
PZ1-Peg5	13.11	15.44
PZ1-Peg8	13.76	16.96
PZ1-SSS	11.72	14.14
DPR-βAla	10.68	13.16
DPR-GSG	10.73	12.73
DPR-SGS	11.46	12.31
DPR-SSS	11.08	12.77

conjugates show a single species. ESI-MS analyses were consistent with the molecular weights calculated for each analog (Table I).

The *fac*-[^{99m}Tc-(H$_2$O)$_3$(CO)$_3$]$^+$ precursor was used to prepare the metallated conjugates in high yield (~90%). These analogs eluted two to three minutes later than their corresponding nonmetallated counterparts, making it possible to collect the ^{99m}Tc-(CO)$_3$-X-Y-BBN(7-14)NH$_2$ conjugates as high specific activity products (Table II). These products demonstrated *in vitro* stability in excess of 24 hours as monitored by RP-HPLC, with no observable degradation or transchelation to serum proteins. This stability was maintained when challenged with incubation in either histidine solution (1 mM) or HSA.

In vitro analysis. All analogs demonstrated high specificity and affinity for the GRP receptor against ^{125}I-Tyr^4-BBN(7-14)NH$_2$ in competitive radioligand cell-binding assays. This is evidenced by the fact that all derivatives exhibit IC$_{50}$ values in the single-digit nanomolar range for both the T47-D and MDA-MB-231 cell lines (Table I, Figures 1 and 2).

The rate of internalization of cell-associated radioactivity was assessed in the T47-D and MDA-MB-231 cell lines (Figures 3 and 4). The apex of internalization occurred between 45 and 120 minutes, when uptake levels reached 69-88% (PZ1=69-83%, DPR=80-88%) and 34-69% (PZ1=34-50%, DPR=50-69%) of all cell-associated radioactivity in the T47-D and MDA-MB-231 cell lines, respectively. This level of internalization remained relatively constant for subsequent time points, with no significant efflux of radiotracer observed over a 90-minute period (PZ1=92-94% and 80-89%, DPR=84-97% and 88-95% in the T47-D and MDA-MB-231 cell lines respectively).

In vivo biodistribution. All analogs were screened in CF-1 mice at 1 hour *p.i.* to provide an initial assessment of GRP receptor-targeting capacity (Figure 5). The highest levels of accumulation in GRP receptor-positive pancreatic tissue were demonstrated by the DPR analogs (12.2-15.0±0.7-2.7% ID/g). Excluding the ^{99m}Tc-(CO)$_3$-PZ1-βAla-BBN(7-14)NH$_2$ conjugate, whose pancreatic uptake rivaled that of the DPR compounds (8.5±2.2% ID/g), the PZ1 derivatives demonstrated relatively poor uptake by the pancreas (0.8-4.3±0.2-0.7% ID/g).

Table III. *^{99m}Tc-(H$_2$O)(CO)$_3$-DPR-Y-BBN[7-14]NH$_2$ tumor-to-background ratios at 24 hours post-injection.*

Organ	GSG	SGS	SSS
Blood	4.4-8.3	1.7-2.4	2.9-3.5
Liver	2.2-4.2	0.7-1.0	1.7-2.1
Kidneys	1.0-1.8	0.5-0.7	0.8-0.9
S. and L. intestines	2.3-4.8	1.0-2.1	1.3-2.7
Muscle	3.2-6.0	1.2-1.7	2.5-3.0
Bone	1.3-2.4	1.0-1.3	1.1-1.3
Pancreas	0.8-1.5	0.4-0.6	0.7-0.9

Based upon these results, ^{99m}Tc-(CO)$_3$-PZ1-βAla-BBN(7-14)NH$_2$ and the ^{99m}Tc-(H$_2$O)(CO)$_3$-DPR-Y-BBN(7-14)NH$_2$ series of conjugates were selected for further analysis at 1, 4, and 24 hours *p.i.* in CF-1 and tumor-bearing SCID mice (Figures 6 and 7). The number of GRP receptor sites per cell is significantly higher in the T47-D cell line (36,000) when compared with the MDA-MB-231 cell line (2,276) (27, 28). This served as the impetus for the selection of the T47-D line for use in the evaluation of the *in vivo* biodistribution and imaging capability of the various ^{99m}Tc-(CO)$_3$-X-Y-BBN(7-14)NH$_2$ conjugates.

The accumulation and retention of radioactivity in target pancreatic (CF-1=10.0-16.9±1.2-2.5 and 0.7-1.2±0.1% ID/g at 1 and 24 hours *p.i.*, respectively) and tumor (2.0-3.7±0.4-1.8 and 0.5-1.5±0.1-1.7% ID/g at 1 and 24 hours *p.i.*) tissues was highest among the DPR analogs containing amino acid

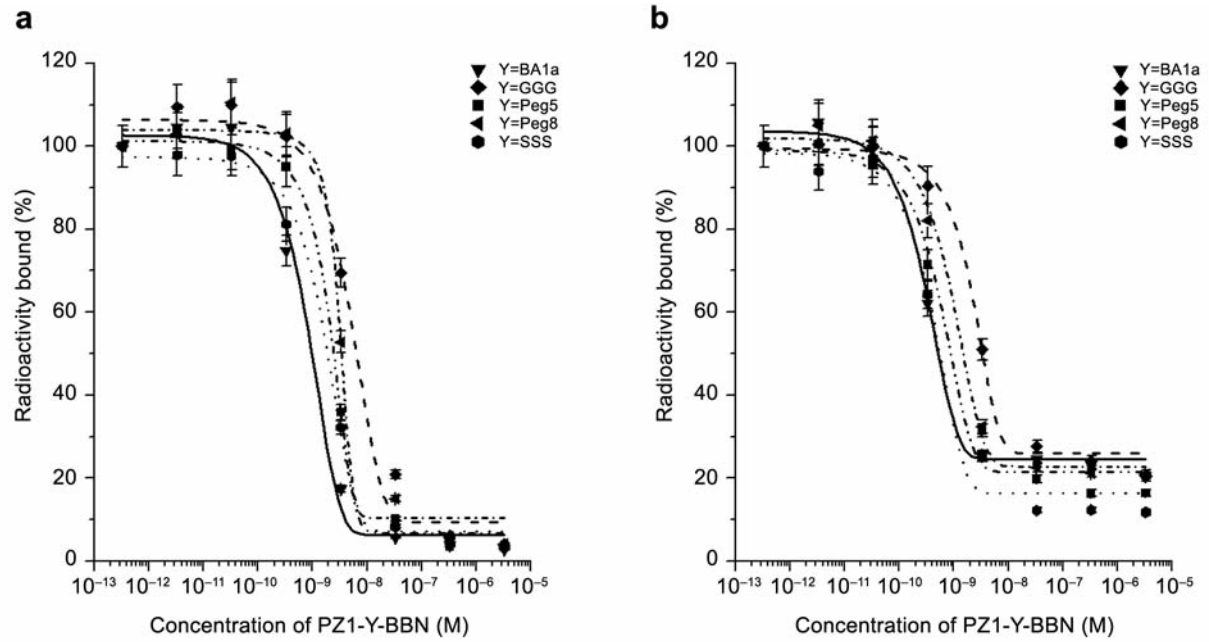

Figure 1. *PZ1-Y-BBN(7-14)NH$_2$ IC$_{50}$ analysis in (a) T47-D and (b) MDA-MB-231 cells (n=3).*

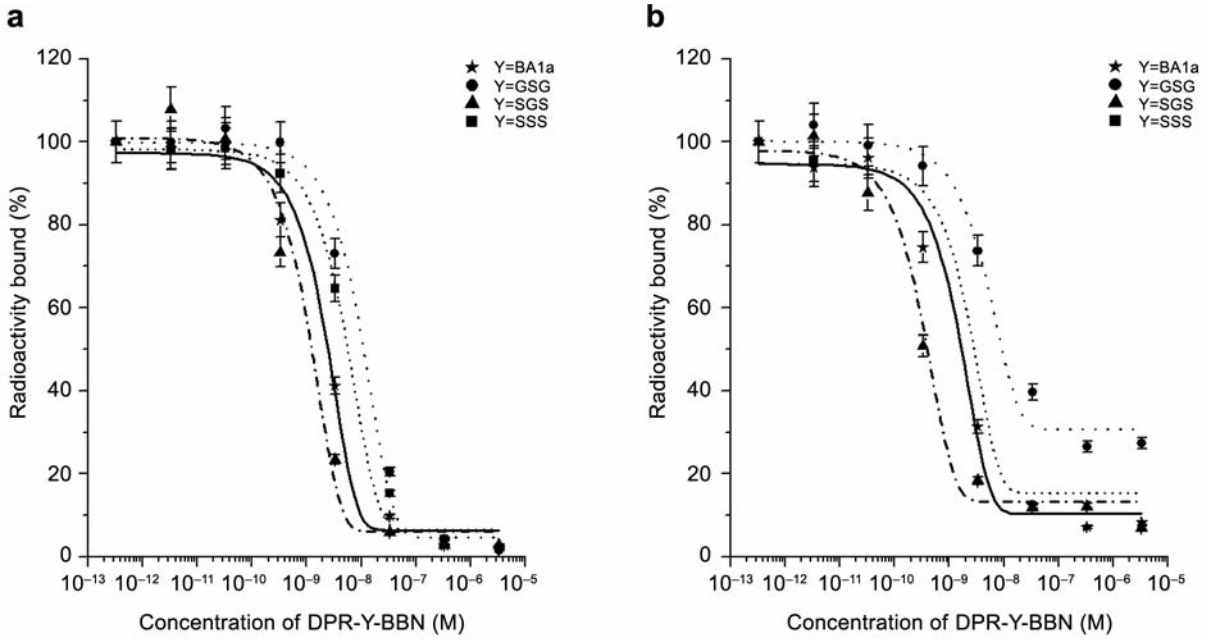

Figure 2. *DPR-Y-BBN(7-14)NH$_2$ IC$_{50}$ analysis in (a) T47-D and (b) MDA-MB-231 cells (n=3).*

spacer sequences. The remaining tissues demonstrated low levels of uptake due to the efficient clearance of these radioconjugates from the bloodstream *via* the renal-urinary system. The opposite trend was observed for the βAla derivatives, which exhibited lower pancreatic (CF-1=8.1-9.3±1.0-1.5 and 0.1-0.8±0.1% ID/g at 1 and 24 hours *p.i.*, respectively) and tumor (1.1-2.8±0.5-1.2 and 0.4-0.8±0.3-0.5% ID/g at 1 and 24 hours *p.i.*, respectively) accretion, and residualization, increased gastrointestinal uptake, and hepatobiliary excretion. Despite the potential for *in vivo*

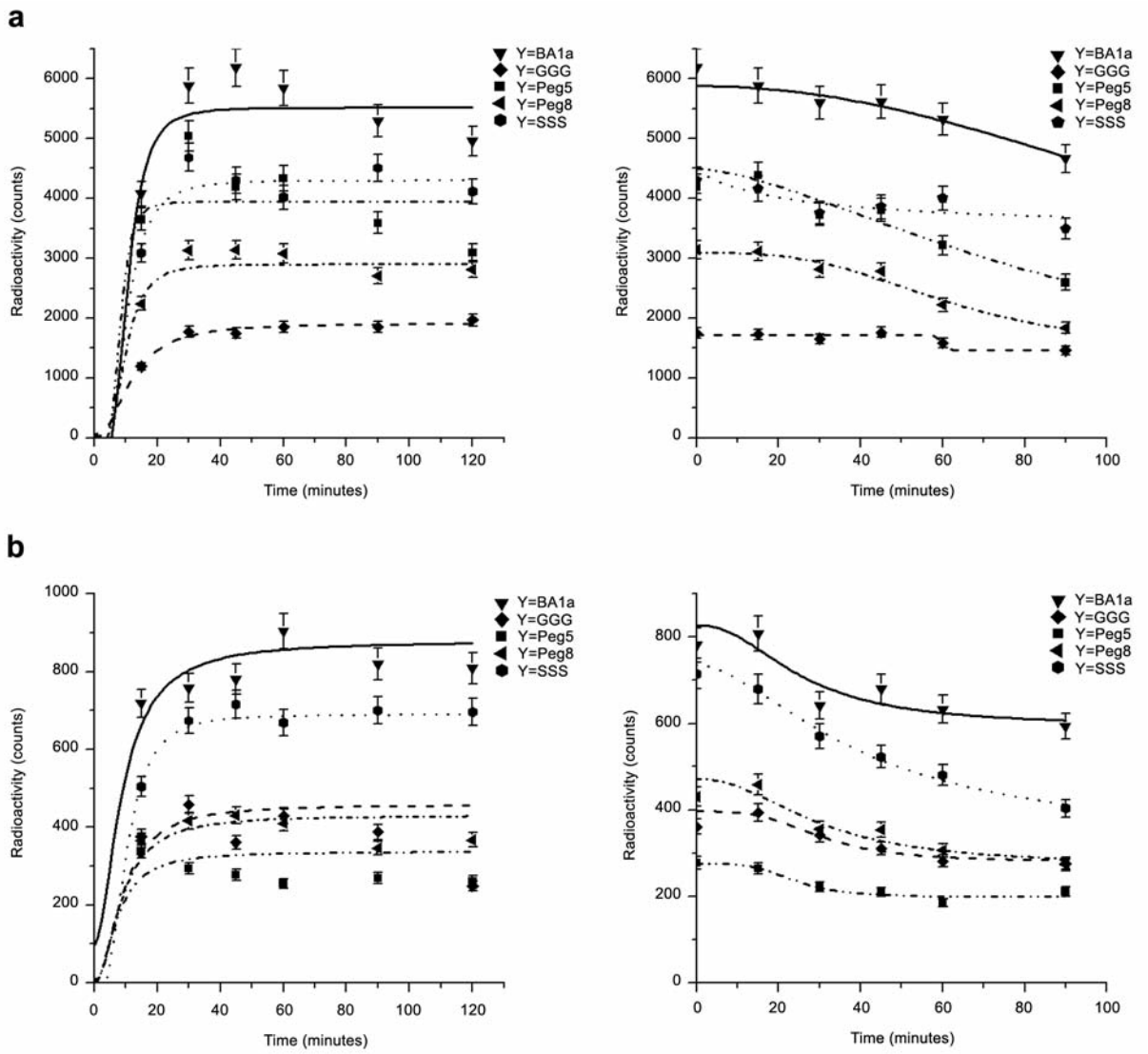

Figure 3. *^{99m}Tc-(CO)$_3$-PZ1-Y-BBN(7-14)NH$_2$ internalization and externalization in (a) T47-D and (b) MDA-MB-231 cells (n=3).*

transligation associated with a bidentate ligand framework, radioactivity in the blood pool remained relatively low, indicating little or no complex formation with serum proteins. Furthermore, the DPR derivatives demonstrated low levels of radioactivity in the stomach at all time points, indicating that there was minimal, if any, *in vivo* dissociation of ^{99m}Tc to ^{99m}TcO[4].

The DPR derivatives containing the GSG and SSS amino acid spacer sequences were selected for imaging studies at 24 hours *p.i.* in T47-D tumor-bearing SCID mice due to both their moderate accumulation and retention in tumor tissue and their rapid elimination from nontarget tissues *via* the renal-urinary system. These characteristics produced favorable tumor-to-background ratios which allowed for the clear visualization of tumor tissue, despite the presence of low levels of background radioactivity (Table III, Figure 8). Although the location and intensity of this background radioactivity fluctuated slightly among these conjugates, the kidneys and the gastrointestinal tract were consistently the predominant sources of this radioactivity at the time of imaging (renal=1.0-1.8 and 0.8-0.9, gastrointestinal=2.3-4.8 and 1.3-2.7 for Y=GSG and SSS, respectively).

Discussion

Interest in developing radiopharmaceutical agents that target the BBN receptor superfamily stems from the overexpression of these receptors, the GRP receptor in particular, on a number of different human cancer types (13, 18, 19). These receptors may be targeted using BBN-based radiotracers,

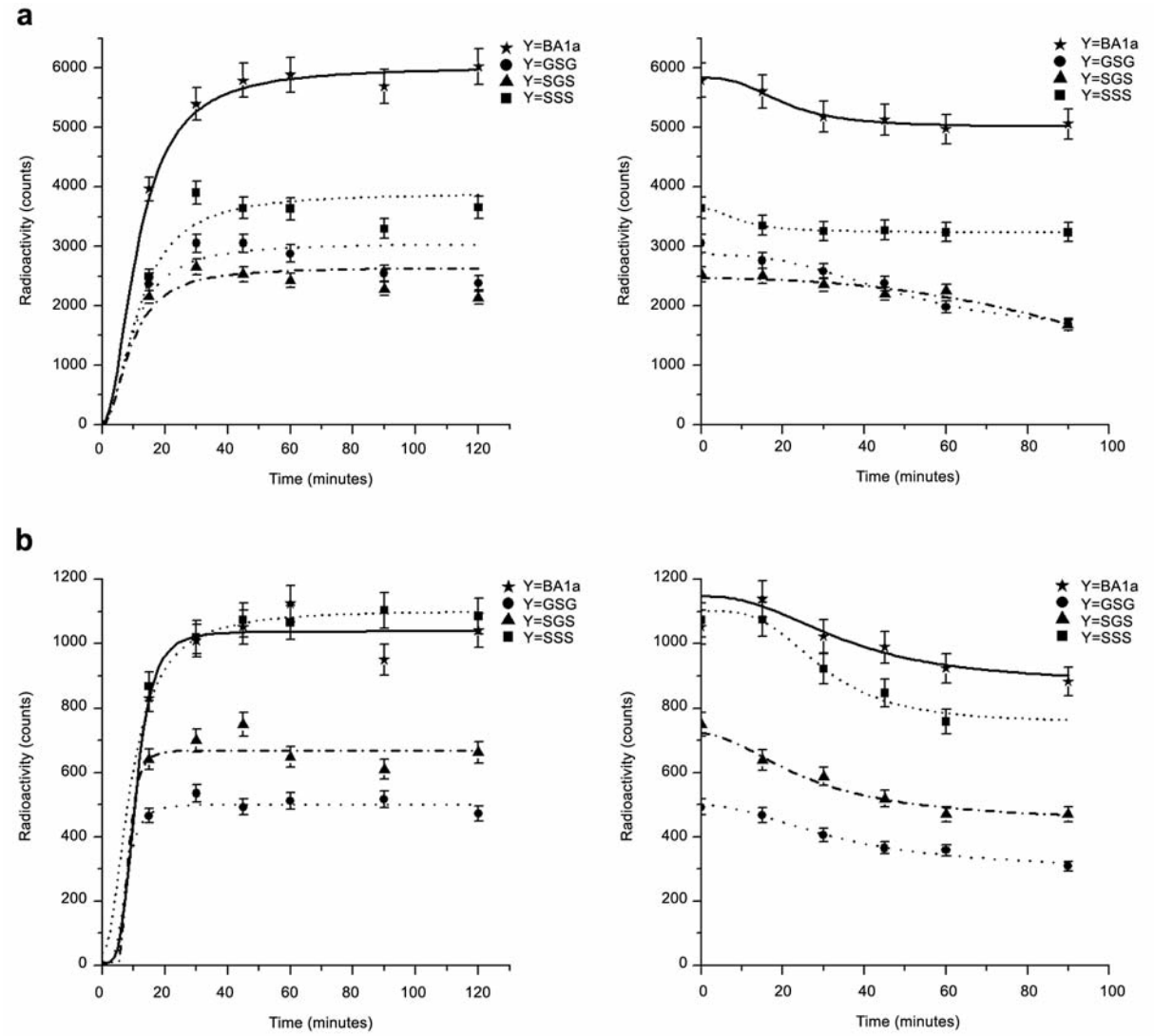

Figure 4. *^{99m}Tc-(H_2O)(CO)$_3$-DPR-Y-BBN(7-14)NH_2 internalization and externalization in (a) T47-D and (b) MDA-MB-231 cells (n=3).*

which have been proven to bind BBN receptors with high affinity and specificity both *in vitro* and *in vivo* (18, 19, 29). In fact, diagnostic and therapeutic radiopharmaceuticals based upon BBN have been shown to hold promise for molecular imaging and treatment of GRP receptor-positive tumors of the breast, prostate, and lung (2, 9, 10, 30, 31). In a series of studies, we synthesized a sequence of ^{99m}Tc-(CO)$_3$-X-Y-BBN(7-14)NH_2 conjugates and analyzed the influence of the bifunctional chelating agent (BFCA), X, and the pharmacokinetic modifier, Y, on the binding affinity, internalization, externalization, *in vivo* biodistribution, and resulting scintigraphic image.

Both the PZ1 and DPR series of conjugates demonstrated very high affinity and selectivity for the GRP receptor *in vitro*. However, the affinity of the PZ1 derivatives was frequently higher than that of the DPR conjugates. These slight differences in binding affinity did not appear to affect analog internalization in either cell line as the highest internalization values were consistently exhibited by derivatives containing either the βAla or SSS spacer sequence regardless of the BFCA employed. With respect to conjugate retention, it has been postulated that the incorporation of aliphatic tethering moieties (βAla, Peg5, Peg8) will obstruct lysosomal fragmentation and subsequent conjugation externalization, thereby prolonging the residence time of a derivative in target tissues. However, our *in vitro* results indicate that this is not universally true. While the βAla linker was associated with increased analog residualization, this effect was more pronounced for the DPR conjugate than its PZ1 counterpart. Furthermore, the incorporation of either the

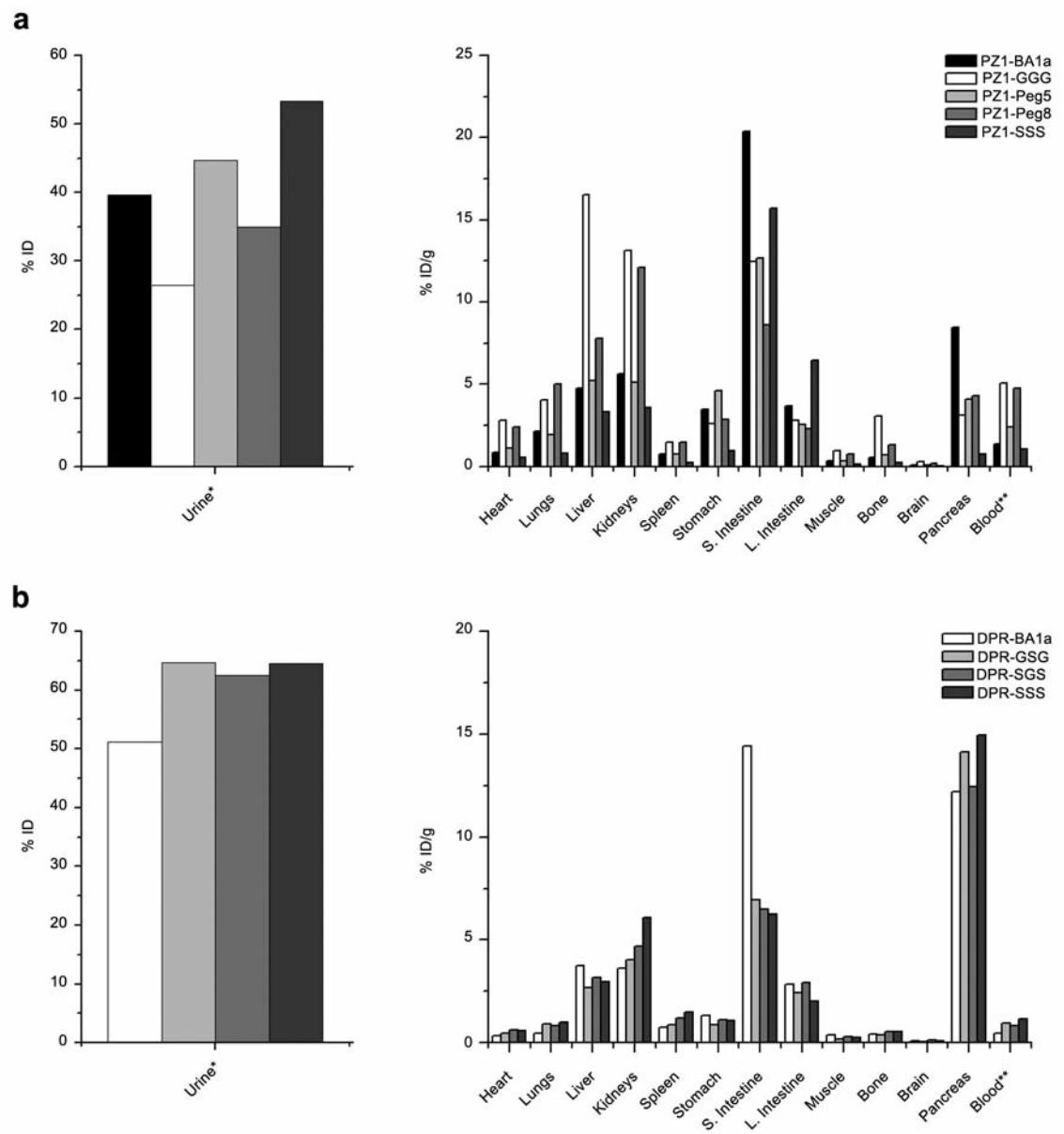

Figure 5. *(a) ^{99m}Tc-(CO)$_3$-PZ1-Y-BBN(7-14)NH$_2$ and (b) ^{99m}Tc-(H$_2$O)(CO)$_3$-DPR-Y-BBN(7-14)NH$_2$ biodistribution screen (%ID/g, n=5) at 1 hour post-injection in normal CF-1 mice. *%ID includes bladder, cage paper and urine. **Assumes 6.5% blood volume by weight.*

Peg5 or the Peg8 spacer sequences did not have any significant effect on derivative retention. This suggests that alternative factors such as conformation, size, hydrophilicity, and/or enzymatic environment of an analog may play an important role in its intracellular retention.

Contrary to the *in vitro* data, the ^{99m}Tc-(H$_2$O)(CO)$_3$-DPR-Y-BBN(7-14)NH$_2$ analogs where Y=GSG, SGS, or SSS consistently demonstrated enhanced target tissue accumulation and superior pharmacokinetic properties when compared to the PZ1 conjugates. This may be attributed to the small size and relatively hydrophilic nature of the DPR ligand and amino acid linkers, which enhances both vascular permeability and renal-urinary elimination. In contrast, the large size and hydrophobic nature of the PZ1 BFCA and aliphatic spacer groups renders these conjugates more susceptible to interaction with plasma proteins as well as hepatobiliary excretion.

The production of tumor-to-background ratios adequate for diagnostic imaging in humans requires radioactivity to be both retained in target tissue and cleared from nontarget tissues. As such, only the DPR conjugates containing amino

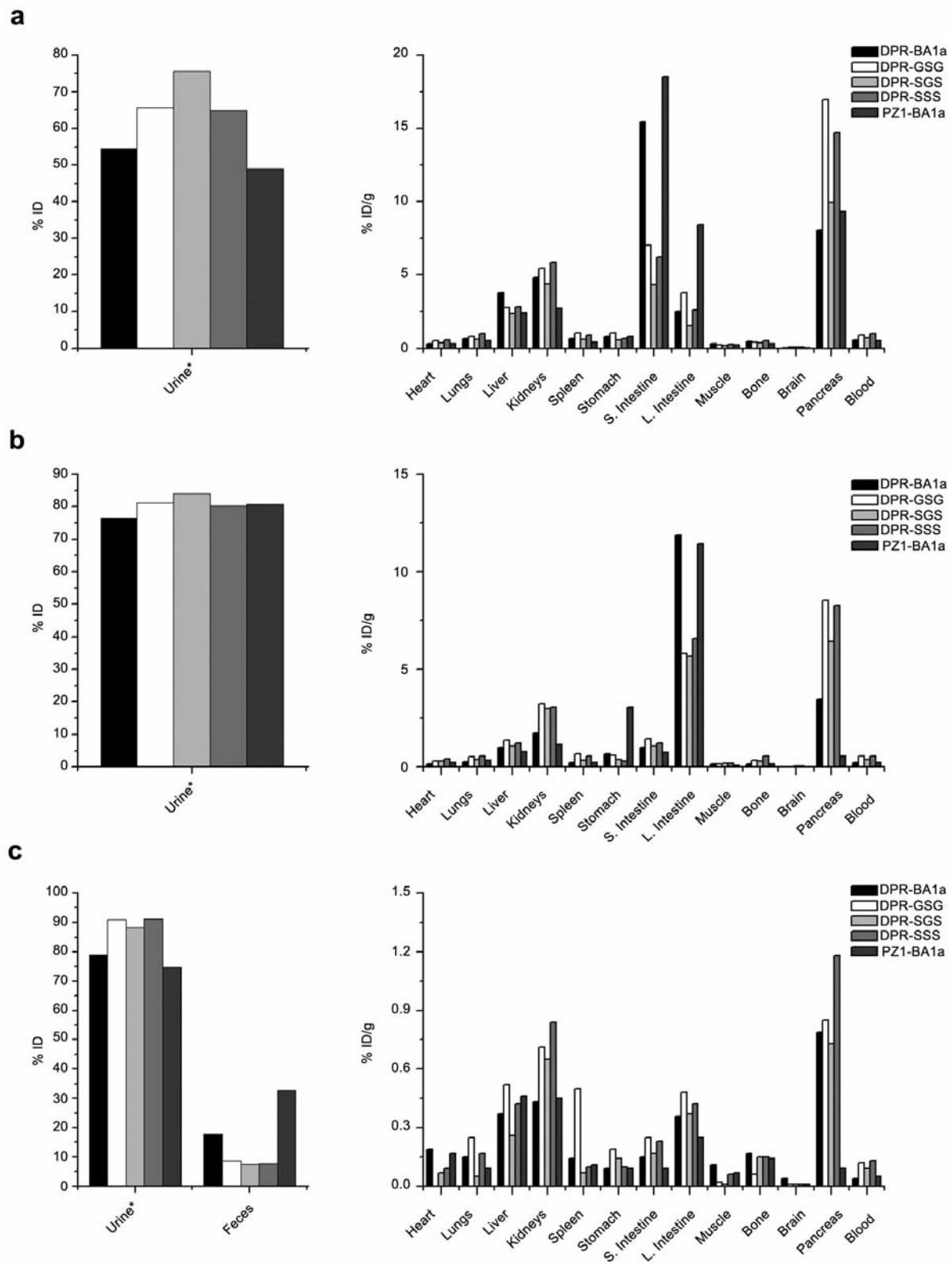

Figure 6. *^{99m}Tc-(CO)$_3$-X-Y-BBN(7-14)NH$_2$ biodistribution data (%ID/g, n=5) at (a) 1, (b) 4, and (c) 24 hours post-injection in normal CF-1 mice. *%ID includes bladder, cage paper and urine. **Assumes 6.5% blood volume by weight.*

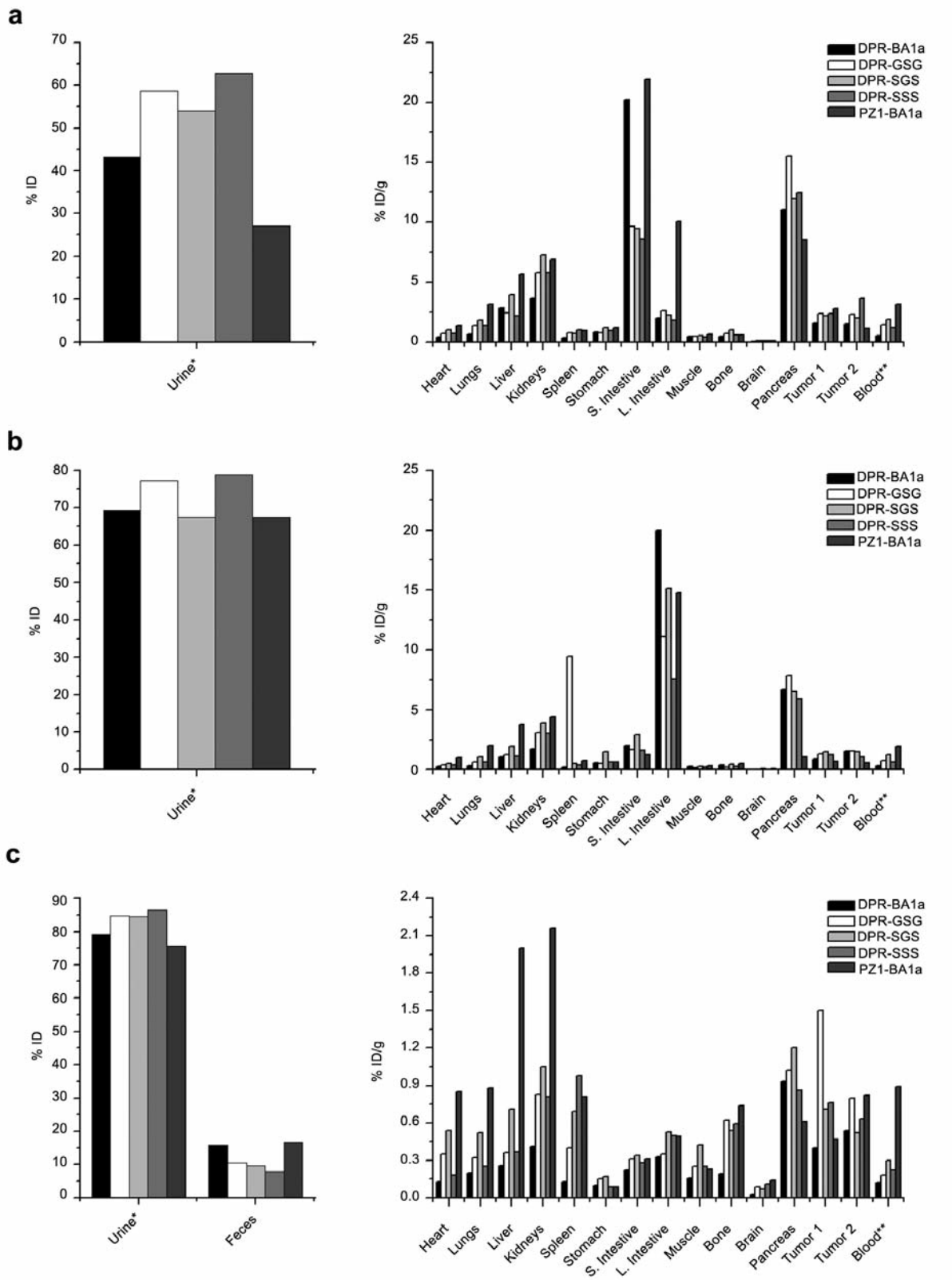

Figure 7. *^{99m}Tc-(CO)$_3$-X-Y-BBN(7-14)NH$_2$ biodistribution data (%ID/g, n=5) at (a) 1, (b) 4, and (c) 24 hours post-injection in T47-D tumor-bearing SCID mice. *%ID includes bladder, cage paper and urine. **Assumes 6.5% blood volume by weight.*

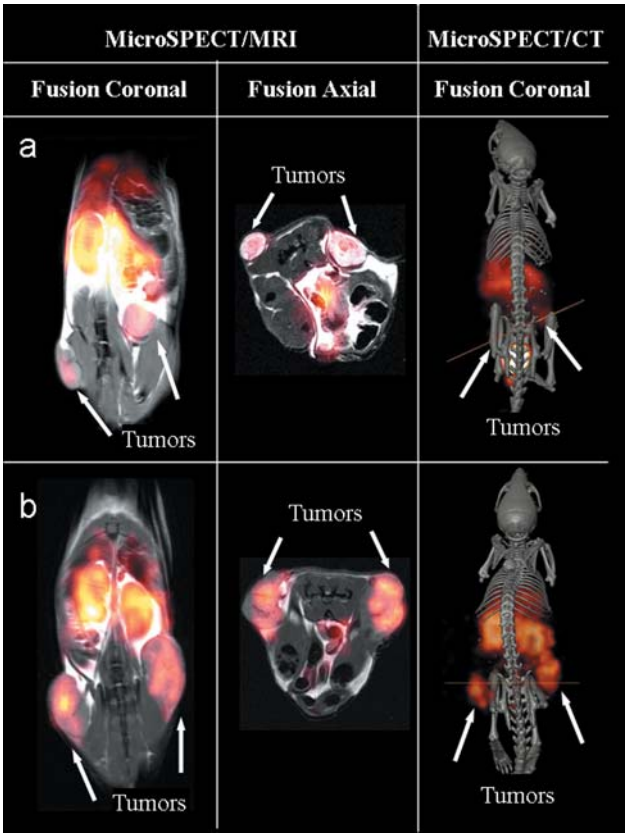

Figure 8. *(a) ^{99m}Tc-$(H_2O)(CO)_3$-DPR-GSG-BBN(7-14)NH_2 and (b) ^{99m}Tc-$(H_2O)(CO)_3$-DPR-SSS-BBN(7-14)NH_2 imaging at 24 hours post-injection.*

acid spacer sequences were considered as potential candidates for imaging studies in T47-D tumor-bearing SCID mice. However, given that at a minimum these ratios should be between 1 and 5, only two of the three candidates, the GSG and SSS derivatives, were selected for further analysis (Table III) (32). The third candidate, ^{99m}Tc-$(H_2O)(CO)_3$-DPR-SGS-BBN(7-14)NH_2, was excluded due to the fact that it demonstrated suboptimal tumor-to-background ratios for a number of organ systems at 24 hours *p.i.* including the heart, liver, kidneys, large intestines, and bone, two of which (liver and bone) are frequent sites of breast cancer metastasis.

The images obtained from the ^{99m}Tc-$(H_2O)(CO)_3$-DPR-Y-BBN(7-14)NH_2 conjugates where Y=GSG or SSS reflected the tumor-to-background ratios calculated from their *in vivo* biodistribution in T47-D tumor-bearing SCID mice, with the ^{99m}Tc-$(H_2O)(CO)_3$-DPR-GSG-BBN(7-14)NH_2 analog exhibiting a slightly lower level of background radioactivity in the gastrointestinal tract, liver, and kidneys. However, despite these subtle differences in biodistribution, the identification of tumor tissue was readily achieved with both derivatives, supporting the hypothesis that radiolabeled ^{99m}Tc(I)-BBN conjugates may be employed to diagnose breast cancer.

BBN-based radiopharamceuticals (^{99m}Tc-RP527, ^{99m}Tc-Cys-Aca-BBN(2-14)NH_2) have been successfully employed to image breast cancer in humans (10, 12). The technetium-99m utilized to radiolabel these agents is in the +5 oxidation state (10, 12). There are certain disadvantages associated with the use of ^{99m}Tc(V) including the difficulty associated with the production of high specific activity and well-defined products, as well as the significant *in vivo* hydrophobicity frequently demonstrated by these analogs which reduce their clinical utility (25, 32). In the +1 oxidation state, technetium-99m can be utilized to produce radiopharmaceuticals demonstrating remarkable *in vitro* and *in vivo* stability against serum-based proteins, as well as superior target tissue uptake and retention when compared to ^{99m}Tc(V)-containing agents (30). Therefore, ^{99m}Tc(I)-based agents could present improved clinical efficacy with respect to breast cancer detection and diagnosis (32). In support of this hypothesis, the biodistribution profile of ^{99m}Tc-N_3S-5Ava-BBN(7-14)NH2 (^{99m}Tc-RP527) in a CF-1 mouse model reveals a somewhat lower level of pancreatic uptake and a significantly higher degree of intestinal accumulation when compared to the ^{99m}Tc-$(H_2O)(CO)_3$-DPR-Y-BBN(7-14)NH_2 conjugates containing amino acid spacer sequences (pancreas=13.8±1.6 *vs*. 10.0-16.9±1.2-2.5% ID/g; intestines=22.9-25.0±7.9-11.8 *vs*. 1.6-7.0±0.2-1.7% ID/g at 1 hour *p.i.*) (33).

In summary, the data presented herein suggests that Tc(I)-labeled targeting vectors may improve the diagnostic utility of these agents as compared to Tc(V)-labeled conjugates. Furthermore, ease of ligand synthesis, conjugation protocols, and radiolabeling techniques satisfies nearly all of the inherent requirements for production of site-directed radiopharmaceuticals of this type.

Acknowledgements

This material is the result of work supported with resources and the use of facilities at the Harry S. Truman Memorial Veterans' Hospital and the University of Missouri School of Medicine. This work was funded in part by grants from the National Institutes of Health and the United States Department of Veterans' Affairs VA Merit Award.

References

1 American Cancer Society. Cancer Facts and Figures 2009 (on line). Available: http://www.cancer.org. Accessed September 20, 2009.
2 Parry JJ, Andrews R and Rogers BE: MicroPET imaging of breast cancer using radiolabeled bombesin analogs targeting the gastrin-releasing peptide receptor. Breast Cancer Res Treat *101*: 175-183, 2007.
3 Lewin JM, D'Orsi CJ, Hendrick RE, Moss LJ, Isaacs PK, Karellas A and Cutter GR: Clinical comparison of full-field digital mammography and screen-film mammography for detection of breast cancer. Am J Roent *179*: 671-677, 2002.

4 Smith RA, Saslow D, Sawyer KA, Burke W, Costanza ME, Evans III WP, Foster RS, Jr., Hendrick E, Eyre HJ and Sener S: American cancer society guidelines for breast cancer screening: update 2003. CA J Clin *53*: 141-169, 2003.

5 Buchberger W, DeKoekkoek-Doll P, Springer P, Obrist P and Dunser M: Incidental findings on sonography of the breast: clinical significance and diagnostic workup. Am J Roent *173*: 921-927, 1999.

6 Davis PL and McCarty KS, Jr. : Sensitivity of enhanced MRI for the detection of breast cancer: new, multicentric, residual, and recurrent. Eur Rad *7*: S289-S298, 1997.

7 Freer TW and Ulissey MJ: Screening mammography with computer-aided detection: prospective study of 12,860 patients in a community breast center. Radiology *220*: 781-786, 2001.

8 Kolb TM, Lichy J and Newhouse JN: Occult cancer in women with dense breasts: detection with screening US-diagnostic yield and tumor characteristics. Radiology *207*: 191-199, 1998.

9 Scopinaro F, Varvarigou AD, Ussof W, De Vincentis G, Sourlingas TG, Evangelatos GP, Datsteris J and Archimandritis SC: Technetium-labeled bombesin-like peptide: preliminary report on breast cancer uptake in patients. CA Biotherapy Radiopharm *17*: 327-335, 2002.

10 Van de Wiele C, Dumont F, Broecke RV, Oosterlinck W, Cocquyt V, Serreyn R, Peers S, Thornback J, Slegers G and Dierck RA: Technetium-99m RP527, a GRP analogue for visualisation of GRP receptor-expressing malignancies: a feasibility study. Eur J Nucl Med *27*: 1694-1699, 2000.

11 Blok D, Feitsma RIJ, Vermeij P and Pauwels EJK: Peptide radiopharmaceuticals in nuclear medicine. Eur J Nucl Med *26*: 1511-1519, 1999.

12 Signore A, Annovazzi A, Chianelli M, Corsetti F, Van de Wiele C, Watherhouse RN and Scopinaro F: Peptide radiopharmaceuticals for diagnosis and therapy. Eur J Nucl Med *28*: 1555-1565, 2001.

13 Reubi JC, Mathias G and Waser B: Co-expressed peptide receptors in breast cancer as a molecular basis for *in vivo* multireceptor tumour targeting. Eur J Nucl Med *29*: 855-862, 2002.

14 Gugger M and Reubi JC: Gastrin-releasing peptide receptors in non-neoplastic and neoplastic human breast. Am J Path *155*: 2067-2076, 1999.

15 Reubi JC, Gugger M, Waser B and Schaer JC: Y1-mediated effect of neuropeptide Y in cancer: breast carcinomas as targets. Cancer Res *61*: 4636-4641, 2001.

16 Halmos G, Wittliff JL and Schally AV: Characterization of bombesin/gastrin-releasing peptide receptors in human breast cancer and their relationship to steroid receptor expression. Cancer Res *55*: 280-287, 1995.

17 Mahmoud S, Staley J, Taylor J, Bogden A, Moreau JP, Coy D, Avis I, Cuttitta F, Mulshine JL and Moody TW: [Psi$^{13, 14}$] Bombesin analogues inhibit growth of small cell lung cancer *in vitro* and *in vivo*. Life Sci *37*: 105-113, 1985.

18 Smith CJ, Volkert WA and Hoffman TJ: Radiolabeled peptide conjugates for targeting of the bombesin receptor superfamily subtypes. Nucl Med Biol *32*: 733-740, 2005.

19 Smith CJ, Volkert WA and Hoffman TJ: Gastrin-releasing peptide (GRP) receptor targeted radiopharmaceuticals: a concise update. Nucl Med Bio *30*: 861-868, 2003.

20 Markwalder R and Reubi JC: Gastrin-releasing peptide receptors in the human prostate: relation to neoplastic transformation. Cancer Res *59*: 1152-1159, 1999.

21 Lane SR, Veerendra B, Rold TL, Sieckman GL, Hoffman TJ, Jurisson SS and Smith CJ: $^{99m}Tc(CO)_3$-DTMA bombesin conjugates having high affinity for the GRP receptor. Nuc Med Bio *35*: 263-272, 2008.

22 Marti N, Spingler B and Schibli R: Comparative studies of substitution reactions of rhenium(I) dicarbonyl-nitrosyl and tricarbonyl complexes in aqueous media. Inorg Chem *44*: 6082-6091, 2005.

23 Schibli R and Schubinger PA: Current use and future potential of organometallic radiopharmaceuticals. Eur J Nucl Med *29*: 1529-1542, 2002.

24 Wei L, Babich J and Zubieta J: Bifunctional chelates with mixed aromatic and aliphatic amine donors for labeling of biomolecules with the $\{Tc(CO)_3\}^+$ and $\{Re(CO)_3\}^+$ cores. Inorganica Chim Acta *358*: 3691-3700, 2005.

25 Hunter KW, Crawford NPS and Alsarraj J: Mechanisms of metastasis. Breast Cancer Res 10, 2008.

26 Koglin N and Beck-Sickinger AG: Novel modified and radiolabelled neuropeptide Y analogues to study Y-receptor subtypes. Neuropeptides *38*: 153-161, 2004.

27 Giacchetti S, Gauville C, De Cremoux P, Bertin L, Berthon P, Abita JP, Cuttita F and Calvo F: Characterization, in some human breast cancer cell lines, of gastrin-releasing peptide-like receptors which are absent in normal breast epithelial cells. Int J Cancer *46*: 293-298, 1990.

28 Yano T, Pinski J, Groot K and Schally AV: Stimulation by bombesin and inhibition by bombesin/gastrin-releasing peptide antagonist RC-3095 of growth of human breast cancer cell lines. Cancer Res *52*: 4545-4547, 1992.

29 Rogers BE, Curiel DT, Mayo MS, Laffoon KK, Bright SJ and Buchsbaum DJ: *In vitro* binding and internalization of an indium-111-labeled bombesin derivative to cells expressing the gastrin releasing peptide receptor. *In*: Technetium, Rhenium and Other Metals in Chemistry and Nuclear Medicine. Nicolini M and Mazzi U (eds.). SGE Editoriali, Padova, Italy, pp. 519-525, 1999.

30 Engel JB, Schally AV, Halmos G, Baker B, Nagy A and Keller G: Targeted cytotoxic bombesin analog AN-215 effectively inhibits experimental human breast cancers with a low induction of multi-drug resistance proteins. Endocr Relat Cancer *12*: 999-1009, 2005.

31 Gali H, Hoffman TJ, Sieckman GL, Owen NK, Katti KV and Volkert WA: Synthesis, characterization, and labeling with $^{99m}Tc/^{188}Re$ of peptide conjugates containing a dithia-bisphosphine chelating agent. Bioconjug Chem *12*: 354-363, 2001.

32 Varvarigou A, Bouziotis P, Zikos C, Scopinaro F and De Vincentis G: Gastrin-releasing peptide (GRP) analogues for cancer imaging. Cancer Biother Radiopharm *19*: 219-229, 2004.

33 Smith CJ, Gali H, Sieckman GL, Higginbotham C, Volkert WA and Hoffman TJ: Radiochemical investigations of ^{99m}Tc-N_3S-X-BBN[7-14]NH_2: an *in vitro*/*in vivo* structure-activity relationship study where X=0-, 3-, 5-, 8-, and 11-carbon tethering moieties. Bioconjug Chem *14*: 93-102, 2003.

Received October 6, 2009
Revised November, 30, 2009
Accepted December 2, 2009